JOURNAL OF COMPUTATIONAL PHYSICS 6, 56–67 (1970)

Iteration Methods for Calculating Self-Consistent Fields in Semiconductor Inversion Layers

FRANK STERN

IBM Watson Research Center,
Yorktown Heights, New York 10598

Received September 19, 1969

Two new methods for attaining convergence in self-consistent field calculations are described. They have been applied to semiconductor inversion layers at finite temperature.

1. INTRODUCTION

In this paper we describe methods for calculating self-consistent fields in semiconductor surface inversion layers, with particular emphasis on the iteration methods used. An inversion layer is a thin ($\approx$100 angstroms thick) layer just inside the surface of a semiconductor, characterized by a conductivity type different from that of the bulk of the sample. For example, the current may be carried by electrons in the inversion layer and by holes in the bulk material. The inversion layer is bounded at the semiconductor surface by a steep potential barrier and within the semiconductor by a strong electric field. The potential well formed in this way has discrete energy levels, each of which is the bottom of a continuum of levels associated with the motion parallel to the surface. The continua are called electric subbands. The existence of quantization in the inversion layer has been well established experimentally [1]. A number of theoretical consequences have been investigated [2], particularly for the electric quantum limit, the case in which only the lowest electric subband is occupied by electrons.

The inversion-layer self-consistent field problem is formally similar to the atomic Hartree self-consistent field problem [3], except that the populations of the subbands depend on temperature and on the position of the Fermi level. Some results on inversion layers at finite temperature have been obtained by Howard [4], who allowed for three occupied subbands. We have extended the calculation to allow for an arbitrary number of subbands and have introduced two new methods for attaining convergence to a self-consistent solution.

The calculation is carried out in the effective mass approximation.[1] The parameters which enter the equations are the effective mass m_3 for motion perpendicular to the surface, the density-of-states mass m_d per constant-energy ellipse in **k**-space for motion parallel to the surface, and the degeneracy factor n_v which gives the number of equivalent valleys. These parameters depend on the orientation of the surface with respect to the crystallographic axes, and on the energy band structure of the semiconductor, as described by Stern and Howard [2]. The reader is referred to Sections 1 and 2 of that paper for the physical background of the problem.

Results of the self-consistent field calculation have been obtained for a number of semiconductors, but in most detail for silicon, on which most experimental work has been done. Results for *n*-type inversion layers on *p*-type silicon, including energy level spacings and populations and the spatial extent of the carrier wave functions, have been obtained for the principal surface orientations and for a range of temperatures, bulk acceptor concentrations, and inversion layer electron populations. These results will be presented in a separate paper. This paper is concerned with the calculation itself.

2. Self-Consistent Field Equations

We want to find self-consistent solutions of the effective-mass-approximation Schrödinger equation

$$P_i''(z) = (2m_{3i}/\hbar^2)[V(z) - E_i]\, P_i(z) \tag{1}$$

with the boundary conditions

$$P_i(0) = 0, \qquad P_i(\infty) = 0, \tag{2}$$

for the envelope function, where i identifies the subband and m_{3i} is the effective mass for motion in the z direction [2]; and of Poisson's equation (in mks units)

$$V''(z) = -(e^2/\epsilon)\left[N_I(z) + \sum_i N_i P_i^2(z)\right] \tag{3}$$

with the boundary conditions

$$V(0) = 0, \qquad V'(\infty) = 0, \tag{4}$$

[1] Corrections to effective-mass-approximation energy levels have been estimated by W. E. Howard (to be published).

where P_i, which is real, is normalized so that

$$\int_0^\infty P_i^2(z)\,dz = 1, \tag{5}$$

and $\epsilon = \kappa_{sc}\epsilon_0$ where κ_{sc} is the dielectric constant of the semiconductor. The quantity in brackets in (3) gives the number of electronic charges per cubic centimeter. The fixed depletion layer charge density contributed by ionized impurities is

$$N_I(z) = N_A - N_D, \qquad 0 < z < w, \tag{6}$$

where N_A and N_D are the acceptor and donor concentrations in the bulk, and w is the depletion layer thickness. The semiconductor surface is the plane $z = 0$, and the z axis points into the semiconductor. We assume that $N_I(z)$ vanishes outside the z interval indicated in (6).[2] The summation in (3) gives the contribution to the charge density made by the electrons in the surface subbands that are the solutions to (1). The number of electrons per unit area in the i-th subband is [2]

$$N_i = a_i \ln\{1 + \exp([E_F - E_i]/KT)\}, \tag{7}$$

$$a_i = n_{vi} m_{di} KT/\pi\hbar^2, \tag{8}$$

where m_{di} is the density-of-states effective mass per constant energy ellipse in the k_x, k_y plane, n_{vi} is the degeneracy factor for the ellipses, K is Boltzmann's constant, T is the absolute temperature, and E_F is the Fermi energy. For inversion layers on silicon surfaces of general orientation, there are three sets of values of the parameters m_{3i}, m_{di}, and n_{vi}; each set will have its own ladder of subbands. For the high-symmetry surfaces we consider, there are only one or two sets of values.

The self-consistent field problem being considered here is that of a semiconductor surface, but the equations which enter are very much like those which enter in atomic self-consistent fields. In those cases the nuclear charge plays the role taken in our case by the fixed depletion charge. The atomic case is simpler than ours in having a fixed N_i for each level i, while in our case the N_i generally vary from iteration to iteration until self-consistency is reached.

3. Iteration Methods

In the standard self-consistent field procedure, one usually starts with an approximate solution, which may be obtained by an analytical approximation

[2] We ignore here variations on the scale of the bulk screening length which occur where the depletion layer meets the semiconductor bulk.

or in some other way, and either directly or through use of (3) and (4) obtains an input potential $V_{\text{in}}(z)$. The Schrödinger equation (1) is then solved with this potential, and the resulting eigenfunctions and eigenvalues are used to obtain an output potential $V_{\text{out}}(z)$ *via* (3). If V_{in} and V_{out} agree within acceptable limits, a self-consistent solution has been found. If not, another round of the iteration procedure must be undertaken, and the principal decision that has to be made is the choice of a new input potential for the next round.

The simplest type of iteration is

$$V_{\text{in}}^{(n+1)}(z) = V_{\text{in}}^{(n)}(z) + f^{(n+1)} W^{(n)}(z), \tag{9a}$$

$$W^{(n)}(z) = V_{\text{out}}^{(n)}(z) - V_{\text{in}}^{(n)}(z), \tag{9b}$$

where the superscript labels the round. The factor f, here independent of z, normally lies in the range 0 to 1. A small value gives smooth but slow convergence, while a value close to 1 gives rapid convergence in some cases, but leads to diverging results in others. Experience with a particular problem often is a good guide which allows a choice of f that avoids both divergence and excessively slow convergence. We call this iteration procedure the fixed-convergence-factor method.

We use as a measure of convergence the value of $W^{(n)}(z)$ with the largest magnitude, and call it w_n. Note that w_n may be either positive or negative. When a fixed convergence factor f is used, the values w_n often follow a geometric progression with increasing n. We find that convergence of subsequent rounds is generally improved by using

$$f^{(n+1)} = f^{(n)}/(1 - r), \tag{10}$$

where $r = w_n/w_{n-1}$, and where we have assumed that $f^{(n-1)} = f^{(n)}$. Thus if the convergence is slow, and r is close to 1, the new value of f will be substantially larger than the previous value. If the convergence is rapid, r will be close to 0, and f remains relatively unchanged. When the solution is diverging, the procedure of (10) can lead to extreme values for the new f. We have chosen to restrict f to the range between 0.1 and 0.8. We call this extension of the use of (9) the extrapolated-convergence-factor method. An example of the use of this method will be given below.

The procedure just described gives satisfactory convergence in most cases, and provides faster convergence than a procedure with a fixed value of f if the initial value of f was not well-chosen. Other methods of varying f can also be used, such as starting with an initial value of the convergence factor, and then increasing the value toward 1 according to a predetermined schedule [5]. This may lead to difficulty unless the initial value of f, and the schedule for changing it, are wisely

chosen. One would like to have a method which does not need to rely on intuition and experience. The extrapolated-convergence-factor method described in the previous paragraph is one attempt in that direction, although it is still quite empirical.

There have been other convergence procedures described in the literature [6–8], among them the method of Pratt [9], recently used by Rudge [10], which uses a different value of f for each value of z, and changes the value of f from round to round by a linear extrapolation based in the results of the two prior rounds.

The method which we have found most satisfactory for self-consistent calculations for inversion layers is the method we shall call the perturbation-iteration method. We deduce the change in output potential to be expected from a change in the input potential, and then find that change which makes the resulting new input potential equal the predicted output potential. The method is based on first-order perturbation theory, and is therefore expected to converge if the starting point is not too far from self-consistency. In our work the perturbation-iteration scheme is generally applied after a few rounds of the simple fixed-convergence-factor method and the extrapolated-convergence-factor method have been used.

To apply the perturbation-iteration scheme, we choose a set of values z at which the input and output potentials are to be evaluated. This grid will normally be a subset of the full grid used in solving Eqs. (1) and (3). If we now assume that a change ΔV_{in} in the input potential is given at each of the major (coarse) grid points, and varies linearly between them, we can use perturbation theory, as described below, to deduce the resulting change in the output potential. We obtain a matrix A such that

$$\Delta V_{\text{out}}(z_i) = \sum_i A_{ij}\, \Delta V_{\text{in}}(z_j). \tag{11}$$

For self-consistency we require that

$$V_{\text{in}} + \Delta V_{\text{in}} = V_{\text{out}} + \Delta V_{\text{out}}\,. \tag{12}$$

After the n-th round of the calculation, the $\Delta V_{\text{in}}^{(n)}$ required to obtain self-consistency in this approximation is

$$V_{\text{in}}^{(n+1)}(z_i) - V_{\text{in}}^{(n)}(z_i) = \sum_j B_{ij}[V_{\text{out}}^{(n)}(z_j) - V_{\text{in}}^{(n)}(z_j)], \tag{13}$$

where the matrix B is the inverse of the matrix (1-A) and 1 here stands for a unit matrix. Values of $\Delta V_{\text{in}}^{(n)}$ at points between the major grid points z_i are found by interpolation.

4. Calculation of The Perturbation Iteration Matrix

To find the change in output potential that results from a change ΔV_{in} in input potential which is specified only at the points z_i, we first write

$$\Delta V_{\text{in}}(z) = \sum_i \Delta V_{\text{in}}(z_i)\, t_i(z), \tag{14}$$

where the triangular functions t_i are defined by

$$\begin{aligned} t_i(z) &= 0, && z < z_{i-1}, \\ t_i(z) &= (z - z_{i-1})/(z_i - z_{i-1}), && z_{i-1} \leqslant z \leqslant z_i, \\ t_i(z) &= (z_{i+1} - z)/(z_{i+1} - z_i), && z_i \leqslant z \leqslant z_{i+1}, \\ t_i(z) &= 0, && z_{i+1} < z. \end{aligned} \tag{15}$$

The z_i are in increasing order as i goes from 1 to N. The range of values of z in which we solve Eqs. (1) and (3) is the range from 0 to ∞, but the numerical integrations only go to a finite value z_N; approximate analytical expressions are used for larger values of z. The first major grid point is taken at $z_1 > 0$, and the value z_0 which enters in the definition of $t_1(z)$ is taken to be 0. The value z_{N+1} which enters in the definition of the last triangular function, t_N, is taken to be infinite.

With these definitions of the t_i, the perturbing potential $\Delta V_{\text{in}}(z)$ vanishes at $z = 0$, has the values $\Delta V_{\text{in}}(z_i)$ at the major grid points z_i, varies linearily between successive points, and is constant for $z \geqslant z_N$. There are, of course, many other possible ways of choosing $\Delta V_{\text{in}}(z)$ between the fixed values at the grid points. The method of linear interpolation we have chosen is the simplest, and also allows the necessary calculations to be carried out quite efficiently.

To calculate the change in output potential which results from the change (14) in the input potential, we use perturbation theory to calculate the changes in the quantities which appear on the right in (3). The energy change of the j-th level produced in first order by the potential energy change (14) is

$$\Delta E_j = \sum_i \Delta V_{\text{in}}(z_i) \int_0^\infty P_j^2(z)\, t_i(z)\, dz, \tag{16}$$

and the corresponding change in the number of carriers in the j-th subband is found from (7) to be

$$\Delta N_j = (\Delta E_F - \Delta E_j)\, D_j, \tag{17}$$

$$D_j = (a_j/KT)\{1 + \exp([E_j - E_F]/KT)\}^{-1}, \tag{18}$$

where a_j is defined in (8). In our calculation the total number of carriers in the inversion layer is held fixed, so that

$$\Delta E_F = \sum_i d_i \, \Delta E_i \,, \tag{19}$$

where $d_i = D_i / \sum_j D_j$.

The change in the j-th wave function produced by (14) is

$$\Delta P_j = \sum_i{}'' \, P_i(z) \int_0^\infty P_i(z) \, P_j(z) \, \Delta V_{\text{in}}(z) \, dz / (E_j - E_i). \tag{20}$$

The double prime on the summation excludes $i = j$, and also excludes all i belonging to a different set of constant-energy ellipses [2]. Matrix elements linking states at different points in the Brillouin zone are expected to be much smaller than those which we retain in (20), because the matrix element between the corresponding Bloch states is much smaller than that for states at the same point in the zone.

The only other quantity which enters in Eq. (3) for the output potential is the thickness w of the depletion layer. That thickness will change when the input potential changes, but the change is small in most cases. It has been taken into account in our calculations, but is omitted from the presentation here to prevent a mass of detail from obscuring the simplicity of the perturbation-iteration method.

We can now write the matrix elements which enter in (11) in the form

$$A_{kl} = \sum_i \mathscr{V}_{ii}(z_k) \, D_i \left\{ \sum_j d_j t_{l,jj} - t_{l,ii} \right\} + \sum_{ij}{}'' \, [(N_i - N_j)/(E_i - E_j)] \, \mathscr{V}_{ij}(z_k) \, t_{l,ij} \,, \tag{21}$$

where

$$t_{l,ij} = \int_0^\infty P_i(z) \, P_j(z) \, t_l(z) \, dz \tag{22}$$

and $\mathscr{V}_{ij}$ is the solution of the Poisson equation

$$\mathscr{V}_{ij}''(z) = -(e^2/\epsilon) \, P_i(z) \, P_j(z) \tag{23}$$

with the boundary conditions (4). With the matrix A given in (21) we proceed as in (13) to find the approximate change in input potential which is expected to lead to a self-consistent solution.

When many subbands are used, the number of times Eq. (23) must be solved is substantially larger than the number of sub-bands. The amount of calculation can be reduced if we approximate $(N_i - N_j)/(E_i - E_j)$ for a fixed i by a constant $\mathscr{R}_i$

and use the closure approximation [11] and the Green's function for Poisson's equation (23). Then the last term in (21) is replaced by

$$\sum_i \mathscr{R}_i[\mathscr{W}_{l,ii}(z_\kappa) - \mathscr{V}_{ii}(z_\kappa)\, t_{l,ii}] \tag{24}$$

where $\mathscr{W}_{l,ii}$ is the solution of the differential equation

$$\mathscr{W}''_{l,ii}(z) = -(e^2/\epsilon)\, P_i^2(z)\, t_l(z) \tag{25}$$

with the boundary conditions (4).

The foregoing procedure gives the new input potential at the major grid points z_κ. We have generally used 20 to 30 major grid points, as opposed to 300 to 1000 points in the numerical integration of the Schrödinger and Poisson equations. An example of a calculation with several values for the number of major grid points is given below.

The locations of the major grid points are chosen so that the straight lines joining them deviate as little as possible from the actual $V(z)$. An approximate choice of the spacing which accomplishes this is found if we note that the maximum deviation between a parabolic arc segment and its chord is given by one-eighth of the product of the change in slope from one end of the segment to the other times the change in the independent variable z from one end to the other. Thus the location of the i-th major grid point is chosen near the value of z for which the field $V'(z)$ satisfies

$$[V'(z_{i-1}) - V'(z)][z - z_{i-1}] = (N - i)^{-2}\, [V'(z) - V'(z_N)][z_N - z], \tag{26}$$

where the z_i have the same significance as in (15). The algorithm (26) places the major grid points closer together for small values of z, where the inversion layer charge density is concentrated, and spaces them more widely at the larger values of z, where most of the charge density is that of the depletion layer ions and where the potential is varying more slowly. An example is given below in Table II.

The criterion we use for convergence of the self-consistent field iterations is that the absolute value of the maximum difference between input and output potential energies be less than the largest of: $KT/2000$, $E_F/10000$, and 0.001 meV. This corresponds to relative errors of the order of 10^{-5}. In practice, we find that the potential converges quite rapidly at the major grid points when the perturbation-iteration scheme is used after a few rounds of the fixed-convergence-factor and the extrapolated-convergence-factor schemes. But between the major grid points the differences can be quite large. This difficulty arises because (13) does not tell us how to interpolate for the values of the new input potential between the major grid points. In our calculation we interpolated linearly for $\Delta V_{\text{in}}/V_{\text{in}}$, rather than for ΔV_{in}, to try to preserve the correct curvature in the potential. Because of the crudeness of this scheme, the differences between V_{out} and V_{in} did not converge

as well between the major grid points as at these points. To remove this difficulty, we used rounds of the fixed-convergence-factor method (9) with $f = 1$ to separate rounds of the perturbation-iteration method after the potential at the major grid points was nearly self-consistent. The combination gave good results.

5. Comparison of Different Iteration Methods

In Fig. 1 we show convergence of a number of different iteration schemes for a particular case, namely an n-type inversion layer with 3×10^{12} electrons/cm^2 on a (100) surface of p-type silicon with 10^{15} acceptors per cm^3, for a temperature of 77°K. The starting potential is obtained by using a variational approximate solution [2], assuming that all the carriers are in the lowest subband. Four of the

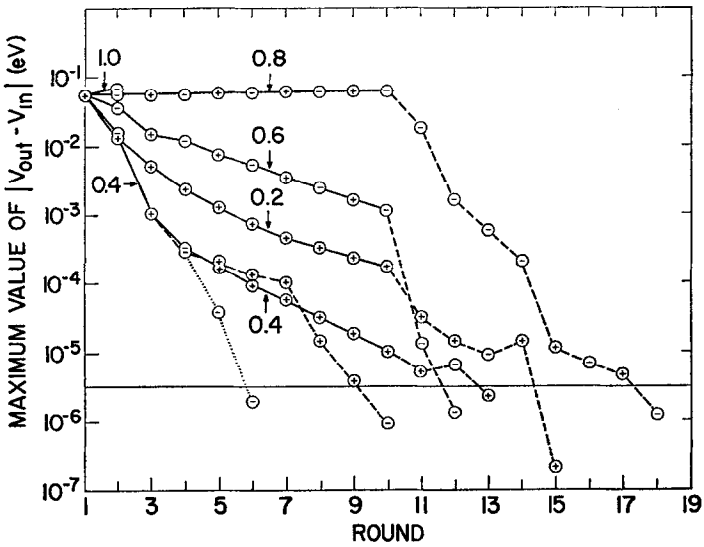

Fig. 1. Comparison of the rate of convergence of different iteration methods for calculating the self-consistent field at 77 °K for an inversion layer on a (001) surface with 3×10^{12} electrons/cm^2 on p-type silicon with 10^{15} net acceptors/cm^3. Nine subbands were explicitly included in the calculation. The input potential for round 1 was obtained from a variational approximation, assuming all the carriers to be in the lowest subband, and led to an extremal value of $V_{out} - V_{in} = 0.053$ eV where V_{in} was 0.189 eV. The circled signs in the figure indicate the sign of $V_{out} - V_{in}$. Solid lines connecting the rounds show that the fixed convergence factor of Eq. (9) was used, with the indicated value of f. Dashed lines show that the extrapolated convergence factor of Eq. (10) was used. The dotted lines indicate use of the perturbation-iteration method. The convergence criterion for this set of calculations was that the greatest absolute value of $V_{out} - V_{in}$ be less than $KT/2000 = 3.3 \times 10^{-6}$ eV, indicated by the horizontal line in the figure.

cases in Fig. 1 use the fixed-convergence-factor scheme to round 10, and the extrapolated-convergence-factor scheme thereafter. We see that the errors, i.e., the maximum values of $V_{out} - V_{in}$, tend to fall off with the number of rounds in a geometric progression. A small value of f, like 0.2 in Fig. 1, leads to slow but steady convergence, while a large value leads to values which are oscillating in sign and increasing slowly in magnitude for $f = 0.8$, and which diverge even more rapidly for case 5 with $f = 1$. A value near $f = 0.4$ gives the best results. At the tenth round we switch to the extrapolated-convergence-factor method, and find that the first four cases then eventually converge. In the sixth case, the fixed-convergence-factor method is used to round three, and the extrapolated-convergence-factor method thereafter. This is seen to be an improvement over the fixed-convergence-factor method. Finally, we introduce the perturbation-iteration scheme after using the fixed-convergence-factor scheme to round three, and the extrapolated-convergence-factor scheme for one round. This gives quite good convergence,

The convergence in the perturbation-iteration scheme improves as the number of major grid points increases, but use of 20 to 30 major grid points appears to give satisfactory results. Use of the closure approximation (24) degrades the convergence somewhat, but satisfactory convergence is obtained even with its use.

TABLE I

Elements of the Matrix B which Relates ΔV_{in} to $V_{out} - V_{in}$, as Used in Eq. (13), for Round 4 of a Case with 10 Major Grid Points; Other Parameters as in the Cases of Fig. 1.

	1	2	3	4	5	6	7	8	9	10
1	1.053	−.008	−.035	−.023	−.007	−.002	−.000	0.000	0.000	0.000
2	0.178	0.988	−.107	−.080	−.032	−.011	−.002	−.000	−.000	−.000
3	0.317	0.010	0.834	−.152	−.077	−.032	−.010	−.002	−.000	−.000
4	0.424	0.067	−.171	0.792	−.141	−.073	−.028	−.008	−.001	−.000
5	0.481	0.127	−.128	−.214	0.804	−.132	−.063	−.020	−.003	−.000
6	0.506	0.166	−.083	−.184	−.208	0.816	−.113	−.044	−.008	−.000
7	0.513	0.185	−.055	−.154	−.191	−.200	0.844	−.078	−.016	−.000
8	0.515	0.192	−.042	−.137	−.174	−.191	−.169	0.886	−.029	−.000
9	0.516	0.194	−.039	−.131	−.166	−.183	−.165	−.128	0.961	−.001
10	0.516	0.195	−.037	−.128	−.163	−.180	−.162	−.126	−.039	0.999

Table I gives the matrix elements of B, the inverse of (1-A), which relates the new ΔV_{in} to $V_{out} - V_{in}$. To keep the table small, we used a case with 10 major grid points, although larger matrices were used in most of our calculations. It is clear from Table I that the new input potential at a given point depends in an important way on the input and output potentials over the entire range of z,

not only on the values near the given point. This has also been noted by Roothan and Bagus for the expansion method [8]. Values of V_{in}, V_{out}, $V_{out} - V_{in}$ and ΔV_{in} for the fourth round of the calculation that led to the matrix of Table I are shown in Table II, as is the value δV_{in} that would have a given self-consistent potential if added to V_{in} [4].

TABLE II

Examples of the Potentials for Round 4 of the Case for which the Matrix B is Given in Table I. All the Potential Energies are in meV. The last Column Gives the Amount that Must be Added to V_{in} to Give the Self-Consistent Potential Energy

i	z_i(Å)	V_{in}	V_{out}	$V_{out} - V_{in}$	ΔV_{in}	δV_{in}
1	15.	65.247	65.433	0.186	0.191	0.186
2	24.	88.563	88.690	0.127	0.141	0.136
3	34.	102.994	103.001	0.006	0.028	0.025
4	47.	113.593	113.679	0.086	0.108	0.100
5	64.	122.169	122.415	0.247	0.265	0.252
6	86.	129.613	129.811	0.198	0.222	0.210
7	115.	136.812	136.798	−0.015	0.027	0.021
8	157.	145.398	145.194	−0.204	−0.142	−0.144
9	239.	160.583	160.299	−0.284	−0.212	−0.210
10	450.	198.222	197.969	−0.254	−0.180	−0.177

The advantage of the perturbation-iteration scheme over the other schemes we have tried is that it converges in fewer iterations and requires less prior experience. The price that must be paid for this is the additional programming required to calculate the matrices A and B, and the additional computing time needed for their numerical evaluation. For 20 major grid points, one iteration round using the perturbation-iteration scheme to calculate the matrices takes about three times as long as one round using the fixed-convergence-factor scheme. We found that the matrix B does not change much from round to round, and that there is no need to calculate it each time. It can be stored, and the only additional operations for the iterations are the multiplications in (13), plus the linear interpolation for $\Delta V_{in}/V_{in}$ between the major grid points. The perturbation-iteration scheme then takes only about 10% longer per round than the fixed-convergence-factor scheme.

The faster convergence obtained with the perturbation-iteration scheme often more than compensates for the increased computing time per round. Further justification for the use of the method is the reduced reliance on trial and error (or intuition and experience) required when it is used.

A method somewhat similar to ours has been developed by Lang [12], who

calls his method the response function method. He expands ΔV_{in} in a series of orthogonal functions, and calculates the corresponding ΔV_{out} by carrying out as many rounds of the self-consistent field scheme as there are terms in the series. The coefficients are then chosen to make the potential as self-consistent as possible. His method requires less programming, but may require more machine time. Since the methods have not been applied to the same problem, no direct comparison of their speed of convergence is possible at present.

The perturbation-iteration scheme has been applied here to a problem which is the analog of the atomic Hartree self-consistent field calculation. But it is also applicable, with appropriate extensions, to the Hartree–Fock and Hartree–Fock–Slater forms of the atomic self-consistent field equations, and probably to calculations on molecules and crystals also. With proper reformulation, the same scheme can also be applied to the expansion method [8] of dealing with the self-consistent field problem.

ACKNOWLEDGMENTS

I am indebted to F. Herman, N. Lang, and W. E. Rudge for discussions of their self-consistent field calculations, and to R. A. Willoughby for discussions of related problems.

REFERENCES

1. A. B. FOWLER, F. F. FANG, W. E. HOWARD, AND P. J. STILES, *Phys. Rev. Lett.* **16** (1966), 901.
2. F. STERN AND W. E. HOWARD, *Phys. Rev.* **163** (1967), 816.
3. D. R. HARTREE, "The Calculation of Atomic Structures," Wiley, New York, 1957.
4. W. E. HOWARD (unpublished).
5. F. HERMAN, private communication.
6. D. R. HARTREE, "The Calculation of Atomic Structures," Sections 5.3.3 and 5.8, Wiley, New York, 1957.
7. F. HERMAN AND S. SKILLMAN, "Atomic Structure Calculations," Ch. 4, Prentice-Hall Engelwood Cliffs, N.J., 1963.
8. Expansion methods, which we do not consider in this paper, are described by C. C.. J. ROOTHAAN AND P. S. BAGUS *in* "Methods in Computational Physics," (B. Alder, S. Fernbach, and M. Rotenberg, eds.), Vol. 2, p. 62, Academic Press, New York, 1963.
9. G. W. PRATT, *Phys. Rev.* **88** (1952), 1217.
10. W. E. RUDGE, *Phys. Rev.* **181** (1969), 1024.
11. L. I. SCHIFF, "Quantum Mechanics," 2nd edition, Section 10, McGraw–Hill, New York, 1955.
12. N. D. LANG, *Solid State Commun.* **7** (1969), 1047.